

# Electronic Structure and Band Gaps in Cationic Heterocyclic Oligomers. Multidimensional Analysis of the Interplay of Heteroatoms, Substituents, Molecular Length, and Charge on Redox and Transparency Characteristics

Geoffrey R. Hutchison,<sup>†,‡</sup> Mark A. Ratner,<sup>\*,‡</sup> and Tobin J. Marks<sup>\*,‡</sup>

Department of Chemistry and the Materials Research Center, Northwestern University, Evanston, Illinois 60208-3113

Received: July 30, 2004; In Final Form: November 22, 2004

Oxidative doping of extended  $\pi$ -conjugated polymers and oligomers produces dramatic changes in optical and electrical properties, arising from polaron and soliton-derived midgap states. Despite the great importance of such changes for materials properties, far less is known about the cationic polaron states than about the neutral, semiconducting or insulating, undoped materials. The systematic, multifactor computational analysis of oligoheterocycles such as oligothiophenes, oligofurans, and oligopyrroles presented here affords qualitative and quantitative understanding of the interplay among skeletal substitution pattern, electronic structure, and the effective band gap reduction on p-doping. A simple linear relation is derived for predicting p-doped oligomer and polymer effective band gaps based on those of the neutral oligomers; this relationship confirms the effectiveness of a “fixed band” approximation and explains the counterintuitive increase of the effective band gap on p-doping of many small band gap oligomers. The present analysis also suggests new candidates for transparent conductive polymers and predicts limiting behavior of ionization potential, electron affinity, and other properties for various polyheterocyclic systems. The results yield insight into materials constraints in electrochromic polymers as well as on p- and n-type conductors and semiconductors.

## I. Introduction

Thin films of  $\pi$ -conjugated organic oligomers and polymers continue to stimulate great scientific and technological interest, stemming originally from the large increases in electrical conductivity accompanying the halogen p-doping of polyacetylene<sup>1</sup> and polymeric phthalocyanines.<sup>2</sup> The oxidative doping process is known to introduce midgap states and structural distortions such as polarons, bipolarons, and solitons, responsible for the dramatic increases in electrical conductivity.<sup>3,4</sup> Because the study of such states is complicated by many factors, including radical lifetime, chemical/thermal stability, and a host of chemical and physical relaxation processes, debate continues as to the exact nature of these states in both isolated molecules and in condensed-state materials.<sup>5–8</sup> In particular, the electronic structures of the different materials are often quite different, with much of the initial physics derived from our understanding of the (unusual) degenerate ground state *trans*-polyacetylene.<sup>9</sup> Second-generation materials now frequently incorporate oligo- or polyheterocycles such as oligo- and polythiophenes and pyrroles, which have nondegenerate ground states. Also, much of the research activity, from both experimental and theoretical standpoints, has been focused on a detailed understanding of the unsubstituted parent oligothiophenes<sup>6,8,10,11</sup> and oligopyrroles,<sup>11,12</sup> with less effort focusing on systematic comparisons across a variety of skeletal substitutions, even though the consequences are of considerable technological importance and may not be intuitively obvious.

A fundamental and challenging issue, therefore, concerns electronic structure/property relationships involving the radical cation states of variously substituted conjugated p-doped oligoheterocycles. In particular, these materials exhibit strong electrochromic red shifts<sup>13</sup> and in some cases have high optical transmissivity throughout the visible portion of the spectrum, affording so-called “transparent” conductive polymers such as poly(3,4-ethylenedioxythiophene) (“PEDOT”).<sup>14</sup> We present here a detailed, directed multidimensional computational chemistry study of neutral and p-doped oligoheterocycles that considers the interplay of the synthetic parameters, oligomer length, heteroatom identity, heterocycle substituents, and oligomer charge in determining energy levels and optical transitions aimed at understanding the general behavior of p-doped oligoheterocycles. We employ density functional theory (DFT) methods to derive ground-state electronic structures, and well-established semiempirical ZINDO/CIS and time-dependent DFT (TDDFT) methods for optical properties. Our previous work demonstrated that both methods are quite accurate and reliable for predicting the band gaps of neutral oligoheterocycles.<sup>15</sup> Both have been employed to model the band gaps and excited states of radical cations as well, with TDDFT demonstrating high accuracy.<sup>16</sup> Use of two methods here also allows confirmation of results to ensure greater reliability, because relatively few detailed experimental optical absorption spectroscopic studies<sup>8,17,18</sup> have been reported for the radical cations of interest, hindering extensive statistical comparisons with experiment.

Because several physical variables are known to govern the electronic structures of conjugated oligoheterocycles, we report here a systematic multidimensional analysis, which varies oligomer chain length, heteroatom identity, heterocycle sub-

<sup>†</sup> New address: Department of Chemistry and Chemical Biology, Cornell University, Baker Laboratory, Ithaca, NY 14853-1301.

<sup>‡</sup> E-mail: G.R.H., grh25@cornell.edu; M.A.R., ratner@chem.northwestern.edu; T.J.M., t-marks@northwestern.edu.

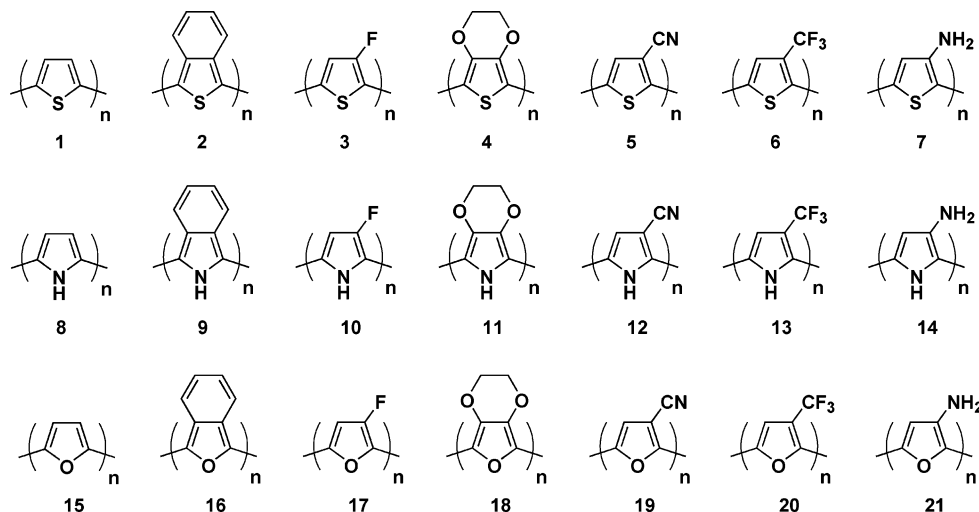


**Figure 1.** Heterocyclic oligomer structures used for multidimensional computational analysis. Note that a diverse variety of substituents are used, including electron donors, electron acceptors, and the widely studied isobenzo (2, 9, 16) and ethylenedioxy (4, 11, 18) substituents. In all cases, oligomer dimensions were varied from 2 to 6 monomer units ( $n = 2-6$ ).

stituent, and charge, and enables reliable statistical analysis of the effect of each factor. Furthermore, the effect of an electron-withdrawing or electron-releasing substituent may differ for a more electron-rich or electron-poor heterocycle, or substituent-induced steric crowding may twist the oligomer chain and hence alter electronic structure scaling with oligomer length. Consequently, implementing a multidimensional analysis can elucidate the interplay of such secondary, or higher order, interactions among structural factors—enabling us to find explanatory qualitative trends in complicated systems. The goal of such an analysis is to identify causal functionality between structural motifs such as heteroatom, heterocycle substituent, etc., and the electronic structure of the oligomer.

It will be seen here that the interplay among these structural factors makes important contributions to the computed electronic structures and excitation energies, illustrating that the effects of heterocycle substituents *can vary dramatically* depending on the charge of the species and/or the nature of the heterocycle. Additionally, it will be shown that the electronic structures of most cationic species studied *are distinctly different* from those expected on the basis of previous theoretical work, with the “midgap” states found to be considerably closer in energy to the occupied molecular orbitals. Finally, we find that the ZINDO/CIS and TDDFT excitation energies are in general agreement for both neutral and cation oligomers and yield a linear relationship between the excitation energies of the neutral and the corresponding monocation species. This relationship predicts a net red shift of band gaps for most molecules but, interestingly, a *blue shift* for smaller gap species. We also suggest several promising candidates for new transparent conducting polymers and for very small band gap cationic systems.

## II. Computational Methods

To treat completely the interplay of oligomer chain length, heteroatom, skeletal substituent, and charge, a total of 210 molecules/oligomers was examined. These encompassed oligomers composed of 2–6 conjugated monomer units, substituted thiophenes, furans, and pyrroles, the parent unsubstituted heterocycles, and those having one of six electronically and sterically diverse substituents, as both neutral and radical cation species, as indicated in Figure 1. The various substituents were chosen as components of known oligothiophenes or oligopyr-

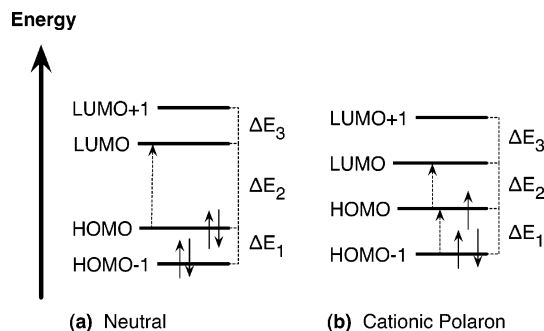


**Figure 2.** Typical energy level diagram and nomenclature for (a) neutral and (b) cationic polaronic  $\pi$ -conjugated oligomers. Dashed arrows indicate the strongest, lowest energy dipole-allowed excitations. Note that in the cationic polaron case, the polaron levels are frequently assumed to be approximately centered in the middle of the band gap of the parent neutral.

roles, or for their established  $\sigma$ - and  $\pi$ -donating or -withdrawing properties.<sup>19</sup> The number of oligomers examined allows statistical analysis of the results, to minimize the effects of small random errors. Furthermore, because a wider range of molecules is examined, one can have greater confidence in estimates of the effect of each principal structural modification.

Full geometry optimization for each molecule was performed using the Q-Chem 2.0 program<sup>20</sup> with the B3LYP hybrid density functional<sup>21</sup> and the 6-31G\* basis set. No symmetry constraints were enforced, and in all cases, several conformations were considered in an attempt to locate the global minimum geometry. All open-shell calculations were performed using unrestricted methods (UDFT and UHF), and spin contamination in the radical cation species was very small ( $\langle S^2 \rangle \leq 0.77$ —less than 3% from the exact expected value, 0.75). For each structure, the two highest occupied and two lowest unoccupied DFT orbital energies were recorded. In the case of the unrestricted open-shell calculations, the spin-orbitals are very close in energy (i.e.,  $<0.1$  eV), and the average is taken for the doubly occupied and unoccupied orbital energies. For facile comparison between the neutral and cationic polaron species, the four levels will be referred to as the HOMO–1, HOMO, LUMO, and LUMO+1 states,<sup>22</sup> respectively, as indicated in Figure 2, even though the polaronic levels are sometimes designated as HOMO, P1, P2, and LUMO in other work.<sup>23</sup> Although HOMO and LUMO eigenvalues from density functional methods cannot be formally

**TABLE 1: Four-Way ANOVA Study of the Principal Factors and Interactions for Computed HOMO–1, HOMO, LUMO, LUMO+1, Primary ZINDO/CIS, and TDDFT Excitation Energies<sup>a</sup>**

effect	HOMO–1	HOMO	LUMO	LUMO+1	ZINDO/CIS	TDDFT
<b>principal factors</b>						
1/ <i>N</i>	X	X	X	X	X	X
heteroatom	X	X	X	X	X	X
substituent	X	X	X	X	X	X
charge	X	X	X	X	X	X
<b>interactions (second order)</b>						
1/ <i>N</i> :heteroatom	X	X		X		X
1/ <i>N</i> :substituent	X	X	X	X	X	X
1/ <i>N</i> :charge	X	X	X	X		
heteroatom:substituent		X	X	X		X
heteroatom:charge		X	X	X	X	
substituent:charge	X	X	X	X	X	X
<b>interactions (third order)</b>						
1/ <i>N</i> :heteroatom: substituent						
1/ <i>N</i> :heteroatom: charge			X	X		
1/ <i>N</i> :substituent: charge	X	X	X	X	X	X
heteroatom:substituent:charge			X	X	X	X
<b>interactions (fourth order)</b>						
1/ <i>N</i> :heteroatom:substituent:charge						

<sup>a</sup> Filled cells (X) indicate factors that are statistically significant for that variable with a 99% confidence level. This analysis summarizes which factors are important in predicting the response of each variable and indicates which factors and interactions should be used for models.

taken as either the ionization potential or electron affinity, respectively,<sup>24</sup> previous studies have shown that B3LYP-derived eigenvalues compare favorably with experimental electron affinities,<sup>25–27</sup> ionization potentials,<sup>25</sup> and band gaps.<sup>28,29</sup>

For excitation energies, computations employed both the semiempirical ZINDO/CIS method<sup>30</sup> with the CNDO program,<sup>31</sup> using the standard active space of 10 occupied and 10 unoccupied orbitals, and full time-dependent DFT (TDDFT) excitation energies with the BLYP functional and the 6-31G\* basis set. These methodologies exhibited excellent correlation with experimental measurements on a set of 60 neutral oligoheterocycles, particularly for longer oligomers.<sup>15</sup> The 10 lowest excitations were calculated using ZINDO/CIS and the first five transitions were calculated initially for TDDFT. If none of the first 5 transitions had significant oscillator strength, then the first 10 transitions were recalculated to ensure that all low-lying transitions with significant (i.e., >0.10) oscillator strength were identified.

Statistical analysis was performed to identify correlations between the molecular structural “principal factors” of heteroatom, substituent, charge, and oligomer size, and the electronic structure and excitation energies computed for the oligomer. To determine which factors and interactions are statistically significant, multidimensional analysis of variance (ANOVA) was used to seek such correlations systematically. These statistically significant factors and second- and third-order interactions were used to construct multivariate linear regression models, which provide specific numeric values describing the consequences of a particular alteration in a structural motif (e.g., oligofuran vs oligothiophene, or neutral vs cation charge). All statistical analyses, including multifactor analysis of variance (ANOVA) and multivariate regressions were performed with the R statistical package, version 1.7.1.<sup>32</sup> The principal factors considered were heteroatom, substituent, charge, and oligomer size. Oligomer size was treated as the reciprocal of the number of monomer units because of well-known approximate “1/*N*” relationship to band gaps for conjugated neutral oligomers having short chain lengths (i.e., 2–6 rings).<sup>33–35</sup> A multifactor ANOVA study was performed on the entire data set, including principal factors, two-, three-, and four-way interactions on the calculated HOMO–1, HOMO, LUMO, and LUMO+1 energy levels, and the ZINDO/CIS and TDDFT transition energies with

highest oscillator strengths. Significant effects were taken as those in the ANOVA model with statistical confidence levels of 99% or higher, as indicated in Table 1 and were used to establish multivariate linear regressions for each of the responses mentioned above, as summarized in Table 2 and explained below.

### III. Results and Discussion

We first compare the patterns of results from the DFT-derived HOMO–LUMO energy gaps and ZINDO/CIS and TDDFT excitation energies. These results are used to derive a predictor for ZINDO/CIS and TDDFT excitations on the basis of a multivariate linear regression of the DFT orbital energies. We then discuss the nature of the midgap states and the variation of their energies with oligomer length, heteroatom, and substituent factors. Next, we discuss the process of building statistical models for interpreting the results, including determining the most useful factors to include and the effects of the interactions on molecular orbital energies and band gaps—these models allow us to explore qualitative and quantitative correlations. Finally, we discuss the relation between computed excitation energies of the neutral and cation species and their consequences for designing novel electrochromic and/or optically transparent conjugated oligoheterocycles.

**A. Comparison of Computational Methods.** As stated above, one reason for computing both ZINDO/CIS and TDDFT excitation energies is to provide an additional measure of reliability for predictions on radical cations. Some caution and problems have been discussed regarding the use of TDDFT methods in large delocalized systems, particularly with higher energy excitations involving ionic character.<sup>36</sup> Both methods demonstrate excellent performance on neutral oligoheterocycles<sup>15</sup> and have been used to predict excitation energies for aromatic radical cations.<sup>16,23</sup> Other work also suggests the productive use of B3LYP-derived HOMO–LUMO energy gaps for estimating optical gaps based on the excellent prediction of experimental ionization potentials and electron affinities from this functional.<sup>26</sup> This method reproduces experimental optical measurements on neutral molecules well, incurring errors similar in magnitude to those of ZINDO/CIS and TDDFT.<sup>29</sup>

Some experimental radical cation optical absorption studies have been performed on the oligomers considered here,

**TABLE 2: Overall Linear Models, Constructed of the Principal Factors and All Second- and Third-Order Interactions for Computed Orbital Energies (HOMO−1, HOMO, LUMO, LUMO+1) and ZINDO/CIS and TDDFT Excitation Energies<sup>a</sup>**

effect	HOMO−1	HOMO	LUMO	LUMO+1	ZINDO/CIS	TDDFT
intercept	−4.92	−4.48	−2.62	−2.57	1.80	1.21
<b>principal factors</b>						
1/N	−4.05	−1.94	2.73	6.21	4.65	5.31
heteroatom (furan)	0.61	0.30	0.57	0.59	0.28	0.19
heteroatom (pyrrole)	1.11	0.86	1.60	1.54	0.75	0.47
substituent (isobenzo)	0.60	0.29	−0.07	0.09	−0.78	−0.21
substituent (fluoro)	−0.41	−0.23	−0.32	−0.23	0.01	−0.32
substituent (ethylenedioxy)	0.63	1.01	0.82	0.95	−0.22	−0.07
substituent (cyano)	−1.37	−1.38	−1.30	−1.17	−0.05	0.06
substituent (trifluoromethyl)	−1.07	−1.15	−0.57	−0.48	0.48	0.36
substituent (amino)	0.41	0.61	0.66	0.77	0.27	−0.15
charge (cation)	−1.22	−1.75	−3.08	−2.16	−0.79	−0.42
<b>interactions (second order)</b>						
1/N: heteroatom (furan)	−1.91	−0.24	0.21	0.15	−0.23	0.70
1/N: heteroatom (pyrrole)	−1.31	−0.12	−0.19	−0.47	−0.89	0.47
1/N: substituent (isobenzo)	0.36	0.86	−1.43	−3.14	−1.45	−2.58
1/N: substituent (fluoro)	0.75	−0.03	0.16	−0.07	−0.31	0.60
1/N: substituent (ethylenedioxy)	0.89	−0.88	−0.74	−1.16	−0.04	−0.23
1/N: substituent (cyano)	1.07	0.64	0.06	−1.16	−0.47	−0.85
1/N: substituent (trifluoromethyl)	0.79	0.44	0.03	−1.00	−0.55	−0.48
1/N: substituent (amino)	1.72	−0.01	−0.35	−1.32	−1.15	−0.68
1/N: charge (cation)	−7.26	−6.80	−8.81	−10.12	−0.39	0.10
heteroatom (furan):substituent (isonaphthyl)	−0.34	0.42	−0.68	−0.44	−0.64	−0.43
heteroatom (pyrrole):substituent (isonaphthyl)	−0.49	−0.16	−0.69	−0.55	−0.25	−0.38
heteroatom (furan):substituent (fluoro)	−0.06	−0.04	−0.14	−0.11	−0.13	0.16
heteroatom (pyrrole):substituent (fluoro)	−0.08	−0.02	−0.14	−0.10	−0.20	−0.03
heteroatom (furan):substituent (ethylenedioxy)	−0.04	−0.06	−0.21	−0.21	−0.04	−0.16
heteroatom (pyrrole):substituent (ethylenedioxy)	−0.37	−0.17	−0.35	−0.24	−0.06	−0.13
heteroatom (furan):substituent (cyano)	−0.33	−0.25	−0.34	−0.30	−0.04	−0.18
heteroatom (pyrrole):substituent (cyano)	−0.35	−0.28	−0.34	−0.40	−0.02	−0.22
heteroatom (furan):substituent (trifluoromethyl)	−0.01	0.04	−0.46	−0.47	−0.46	−0.40
heteroatom (pyrrole):substituent (trifluoromethyl)	−0.05	−0.05	−0.39	−0.46	−0.28	−0.24
heteroatom (furan):substituent (amino)	−0.11	0.16	−0.14	−0.10	−0.42	−0.29
heteroatom (pyrrole):substituent (amino)	−0.28	−0.09	−0.18	−0.15	−0.48	−0.02
heteroatom (furan):charge (cation)	−0.34	−0.23	−0.43	−0.18	−0.09	0.22
heteroatom (pyrrole):charge (cation)	−0.09	−0.19	−0.91	−0.07	−0.23	0.14
substituent (isonaphthyl):charge (cation)	−0.22	0.44	1.06	−0.29	0.87	0.26
substituent (fluoro):charge (cation)	−0.03	−0.02	0.09	0.03	0.23	0.53
substituent (ethylenedioxy):charge (cation)	−0.10	0.13	0.33	0.05	−0.11	0.22
substituent (cyano):charge (cation)	−0.09	0.07	−0.07	−0.09	0.08	0.17
substituent (trifluoromethyl):charge (cation)	0.15	0.22	−0.35	−0.15	−0.37	−0.15
substituent (amino):charge (cation)	−0.19	−0.01	0.03	0.02	−0.38	0.28

<sup>a</sup> Categorical effects are relative to the neutral oligothiophene parent (compound 1). Third-order effects are smaller relative to the second-order interaction effects and are tabulated in Table S2. Values are in eV, except where 1/N is included, in which case values are in eV•(monomer units).

particularly series **1** and **8**.<sup>8,18</sup> Typically, two relatively strong “midgap” absorptions were observed, and for both transitions in the limited number of homooligomers compared, both ZINDO/CIS and TDDFT produce very similar results, illustrated in Figure 3. As the higher energy transitions in the radical cations are typically significantly stronger, we will confine our discussion to these excitations unless noted otherwise. Furthermore, for the purposes of considering optical transparency through the visible spectrum, this transition is both stronger and higher in energy—and therefore more relevant to whether a particular compound will have strong visible optical absorption.

As illustrated in Figure S3, both the DFT and ZINDO/CIS-computed energy gaps compare quite well with the full TDDFT excitation energies for the strongest excitations of the neutral molecules. A systematic skew of −0.5 eV is seen across all neutral molecules for the TDDFT excitation energies, relative to the ZINDO/CIS or B3LYP energy gaps, although the correlation between methods is high. For cationic species, however, the DFT-computed energy gaps yield significant scatter and overall underpredict the TDDFT excitation energies, which typically show a high degree of orbital mixing. ZINDO/CIS shows stronger correlation with the TDDFT excitation

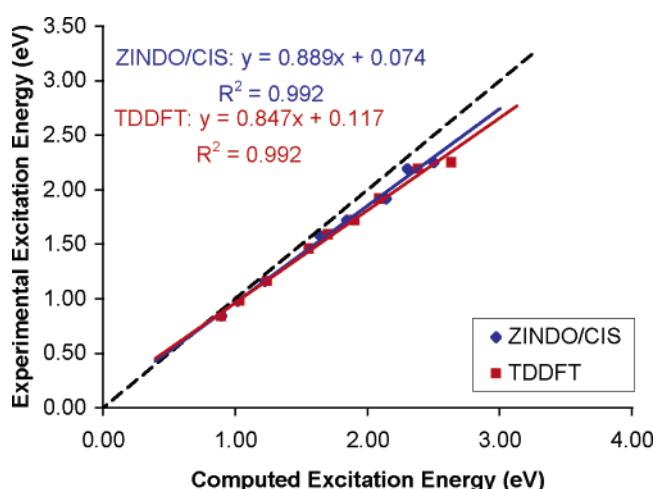


**Figure 3.** Comparison between optical excitation energies computed by ZINDO/CIS or TDDFT and experimental UV/vis spectra for radical cation oligomers in Table S1 (oligomer series **1** and **8**). The dashed line indicates an exact 1:1 correlation. Solid lines indicate the linear regressions for ZINDO/CIS and TDDFT with equations and  $R^2$  values given.



**TABLE 3: Summary of the Multivariate Linear Regressions for Predicting ZINDO/CIS and TDDFT Excitation Energies as Linear Combinations of the DFT Orbital Energies (i.e.,  $\Delta E_{\text{gap}} = C_0 + C_1 E_{\text{HOMO}-1} + C_2 E_{\text{HOMO}} + C_3 E_{\text{LUMO}} + C_4 E_{\text{LUMO}+1}$ )**

method	state	$R^2$	$C_0$ (eV)	$C_1$	$C_2$	$C_3$	$C_4$
ZINDO/CIS	neutral	0.986	+0.158	+0.053	-0.936	+0.799	+0.315
	cation	0.962	+0.246	+0.387	-2.235	+1.625	+0.681
	overall	0.949	+0.022	+0.166	-1.00	+0.331	+0.687
TDDFT	neutral	0.988	-0.535	-0.379	-0.403	+0.454	+0.079
	cation	0.893	-0.134	-0.420	-0.588	+0.352	+0.301
	overall	0.911	-0.525	-0.314	-0.355	-0.113	+0.420

energies but greater scatter than that observed for the neutral molecules, especially at low energies. Of the 210 oligomers, 47 have ZINDO/CIS excitation energies within 0.1 eV of the TDDFT excitation energy (80 within 0.20 eV). The average difference overall between the ZINDO/CIS and TDDFT energies is only 0.31 eV, although the deviation is much smaller for the neutral molecules alone.

Despite the expected limitations of the computed DFT orbital energies in predicting the optical band gaps of cationic molecules, the four frontier orbitals are found to have the highest contribution to both the computed ZINDO/CIS and TDDFT excitations for all molecules. Consequently, they form the basis for an accurate predictor of these excitation energies using a multivariate linear regression. The results are illustrated in Figure S4 and summarized in Table 3, showing that the fitted equations

$$\Delta E_{\text{gap}} = C_0 + C_1 E_{\text{HOMO}-1} + C_2 E_{\text{HOMO}} + C_3 E_{\text{LUMO}} + C_4 E_{\text{LUMO}+1} \quad (1)$$

give accurate and consistent predictions of ZINDO/CIS and TDDFT excitation energies, with average absolute errors of 0.15 eV and 0.13 eV, respectively. These errors are smaller than the reported estimated uncertainties (RMS errors of 0.29 and 0.23 eV for ZINDO/CIS and TDDFT methods, respectively, when compared with experimental absorption  $\lambda_{\text{max}}$  energies) in previous computed/experimental comparisons<sup>15</sup> and illustrate that similar degrees of orbital mixing are computed in both the neutral and cationic molecules. However, the present “four orbital” model itself does not have true physical meaning, because the orbitals in the neutral and radical cation species are quite different in character, and the derived coefficients are a least-squares fit to serve as the best possible predictors of the excitation energies. As an example, many of the coefficients in the overall fits in Table 3 are outside the range of the coefficients fit for the individual neutral or cationic species.

On the other hand, the “four orbital” model is more useful in gaining physical understanding when the neutral and cationic molecules are considered separately, because the coefficients of the linear regression roughly approximate the “configuration interaction” contributions to the orbital mixing upon excitation. As illustrated in Table 3, these coefficients demonstrate that substantial orbital mixing is portrayed by TDDFT, with the HOMOs and LUMOs slightly dominating in the neutral molecules:

$$\Delta E_{\text{gap}} = -0.535 - 0.379 E_{\text{HOMO}-1} - 0.403 E_{\text{HOMO}} + 0.454 E_{\text{LUMO}} + 0.079 E_{\text{LUMO}+1} \quad (2)$$

and the singly occupied HOMO level and LUMO states important in the cationic species:

$$\Delta E_{\text{gap}} = -0.134 - 0.420 E_{\text{HOMO}-1} - 0.588 E_{\text{HOMO}} + 0.352 E_{\text{LUMO}} + 0.301 E_{\text{LUMO}+1} \quad (3)$$

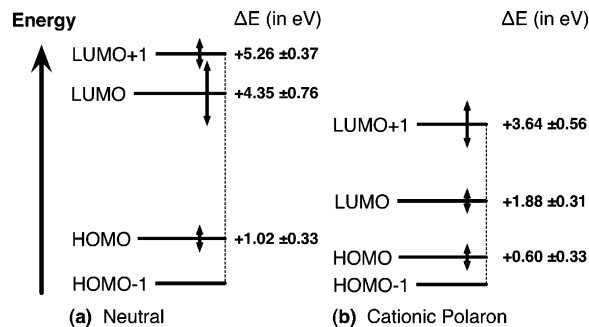


**Figure 4.** Plot of average DFT frontier orbital energy levels for (a) neutral and (b) cationic oligoheterocycles, relative to the HOMO−1 levels. Numbers indicate the average position of the energy levels relative to the HOMO−1 and the standard deviation due to other effects such as oligomer length, heteroatom, and heteroatom substituent (indicated by the scale of the arrows). The HOMO−1 levels also vary as a function of these factors, particularly in going from the neutrals to cations (by  $\sim 3.2$  eV on average). These energy shifts are ignored for the present comparison of the *relative* positions of the orbital energies.

which largely matches the TDDFT configuration interaction coefficients for both species. The HOMO  $\rightarrow$  LUMO+1 transition is formally dipole-disallowed, due to the symmetry of the molecular orbitals, so the relative balance between  $E_{\text{LUMO}}$  and  $E_{\text{LUMO}+1}$  coefficients in eq 3 is strongly indicative of mixing in the unoccupied levels. The picture from ZINDO/CIS reveals significantly less mixing, as the coefficients for the HOMO and LUMO states dominate for both the neutral and cationic molecules. Again, due to the diversity of the compounds considered and the mixing of orbitals beyond the four frontier levels, these coefficients do not have direct physical meaning. However, the high level of correlation between eqs 2 and 3 and the computed TDDFT excitation energies across some 105 oligomers of each class implies that the nature of the optical excitations are remarkably consistent across the entire set.

**B. Molecular Orbital Energy Levels.** As mentioned earlier, Figure 2 illustrates the standard picture of the “midgap” states introduced upon doping. In particular, this picture derives from one-electron, tight-binding approaches, such as the SSH Hamiltonian.<sup>4</sup> These models place the midgap states symmetrically in the center of the band gap, and typically assume a fixed band approximation. The “fixed band” approximation assumes that in the limit of valence and conduction bands, the transition from neutral to cationic species does not alter the relative positions of either band edge but simply introduces the two midgap defect states that previously formed the top of the valence band and the bottom of the conduction band, respectively. Other studies<sup>37</sup> have explained asymmetric polaron states (i.e., not in the middle of the band gap) by single-particle effects, in that distortions of the carbon backbone induced upon polaron formation should affect LUMO energies less, because these have significant participation from the heteroatoms.<sup>7,38</sup> This picture would place the midgap states *above* the center of the gap and predict a significant heteroatom effect on the position of the midgap states, in addition to the obvious effect of oligomer length.

As Figure 4 illustrates, the positions of the midgap states in the present radical cations on average are predicted to be energetically *much closer to the occupied states* than to the unoccupied states. Since density functional methods explicitly include electron correlation, this is not simply a question of single-particle effects. Furthermore, the ANOVA shows that oligomer length, heteroatom, and substituent strongly influence the position of the midgap states. As an example, Figure S5 illustrates the energy levels for oligomer series **1** and **2** as neutral

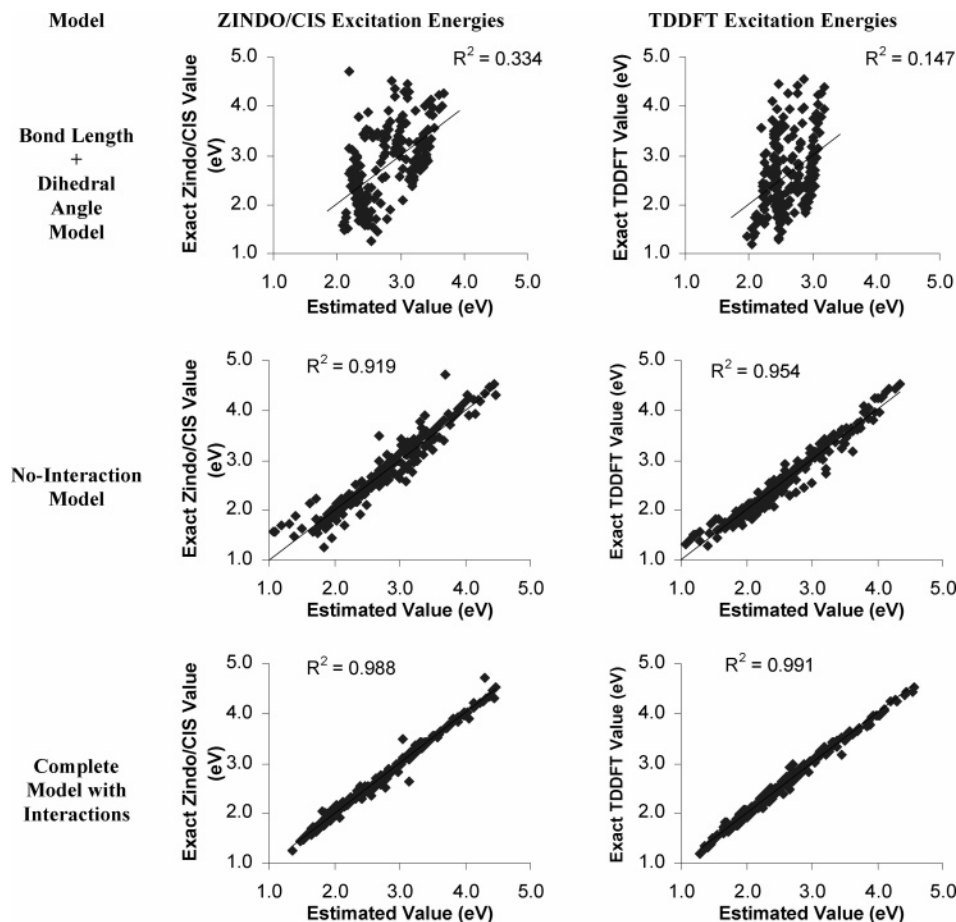
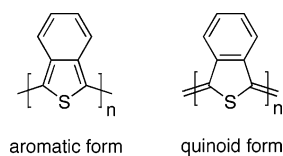


**Figure 5.** Comparison of the improvement in statistical models (as described in the text) in fitting the computed ZINDO/CIS and TDDFT excitation energies of the oligomers in Figure 1. Note that the complete model including interactions not only decreases the magnitude of errors on average, but also the number of poorly modeled species showing significant deviations.

and radical cations. Structure **2** is well-known to have significant quinoidal character arising from the isobenzo substituent,<sup>39–41</sup> and this gives midgap states much closer to the LUMO+1 state than in compound **1**.



Furthermore, the statistical analysis shows that introducing furan or pyrrole rings, on average, increases the gap between the HOMO–1 and HOMO levels (+0.103 and +0.034 eV for furan and pyrrole heterocycles, respectively) and increases the gap between the LUMO and LUMO+1 (+0.186 and +0.658 eV for furan and pyrrole, respectively). The heterocycle substituents that have the greatest influence on the midgap states include cyano, amino, ethylenedioxy, and isobenzo substituents. The latter, as observed in cation **2**<sup>+</sup>, effects an increase in the HOMO–1/HOMO gap (+0.103 eV) but a decrease in the HOMO/LUMO and LUMO/LUMO+1 gaps (–0.164 and –1.18 eV, respectively), likely arising from the highly quinoidal nature of the C–C  $\pi$ -backbone induced by the isobenzo substituent. The amino and ethylenedioxy substituents, on the other hand, depress the HOMO–1/HOMO gap (–0.374 and –0.118 eV, respectively) and the LUMO/LUMO+1 gap slightly (–0.085 and –0.17 eV, respectively), likely due to the  $\pi$ -electron-donating character of these substituents. For example, these two substituents are accompanied by longer C–C formal single

bonds in the oligothiophene cations at the oligomer termini (i.e., more aromatic than quinoidal character), compared to unsubstituted cationic oligothiophenes or series **3**, **5**, or **6**.

**C. Statistical Models: Building and Use.** The process of interpreting the results of a multidimensional/multifactor study such as this is greatly facilitated by statistical analysis, such as multivariate regression and multifactor ANOVA, as illustrated above. Such methods facilitate data exploration and discovery of qualitative and quantitative trends. However, in some cases, additional factors may be important in describing the response, for example, excitation energies. Previous work suggested<sup>41,42</sup> that bond length alternation may be an important factor in describing the HOMO–LUMO gap of  $\pi$ -conjugated oligomers, including oligoheterocycles such as oligopyrroles and oligothiophenes. This follows by analogy to polyacetylenes, where zero bond length alternation produces an intrinsic metal or to a modified particle-in-a-box model which describes the band gaps of oligo- and polyheterocycles, where the band gap at infinite length derives from the amplitude of the potential energy causing bond length alternation.<sup>33,35</sup> Additionally, if the inter-ring dihedral angle is large, then the effective conjugation length of the oligomer is reduced and the excitation energies should be larger. However, when these two effects (bond length alternation and dihedral angle) are used to predict ZINDO/CIS or TDDFT excitation energies, there is poor correlation, as illustrated in Figure 6 (the  $R^2$  values for the models are 0.334 and 0.147, respectively), even though both factors are found to be statistically significant. Because many of the molecules have very similar degrees of bond length alternation and relatively

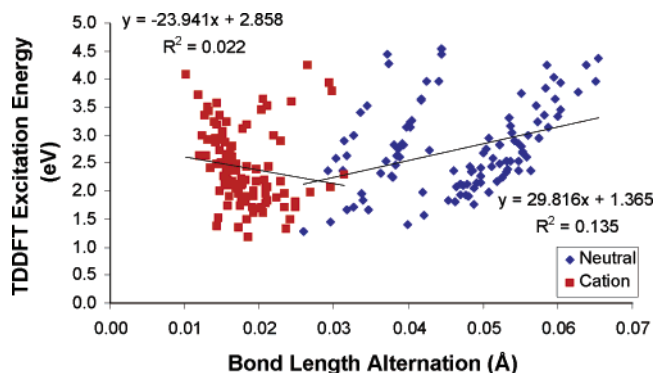


**Figure 6.** Correlations between C–C bond length alternation along the carbon  $\pi$ -backbone of all oligomers in Figure 1, and the corresponding computed TDDFT excitation energies for neutral and cationic species. In general, the excitation energies of the neutral species decrease with decreasing bond length alternation, showing three groups of such decreasing behavior. In contrast, the reverse is true for cationic species, although correlations are weak due to the larger variance.

flat conformations, neither factor varies greatly in comparison to the wide range of excitation energies. Furthermore, smaller bond length alternation is loosely correlated with smaller

excitation energies in neutral oligomers (presumably due to increased delocalization). However, the inverse is true in the cationic oligomers, presumably because less geometric distortion implies the positive charge is more fully delocalized over the entire molecular structure.

The weak correlations indicate that the use of calculated geometric factors such as bond length alternation and dihedral angles as predictors of optical band gaps or other molecular electronic structure properties is inadequate for two reasons. First, as indicated by the low  $R^2$  values, these geometric factors are inaccurate predictors of such electronic structure properties. Second, for rational synthetic design of novel oligomers, these geometric factors are not known a priori, whereas structural factors such as oligomer length or substitution patterns are—thus bond length alternation and dihedral angles would need to be estimated/computed for each hypothetical oligomer under consideration before using these values in any predictive model, whereas the former step is unnecessary for structural characteristics. Because bond length alternation and dihedral angles can be thought of as some function of molecular structure characteristics such as heteroatom, substituent, oligomer length,

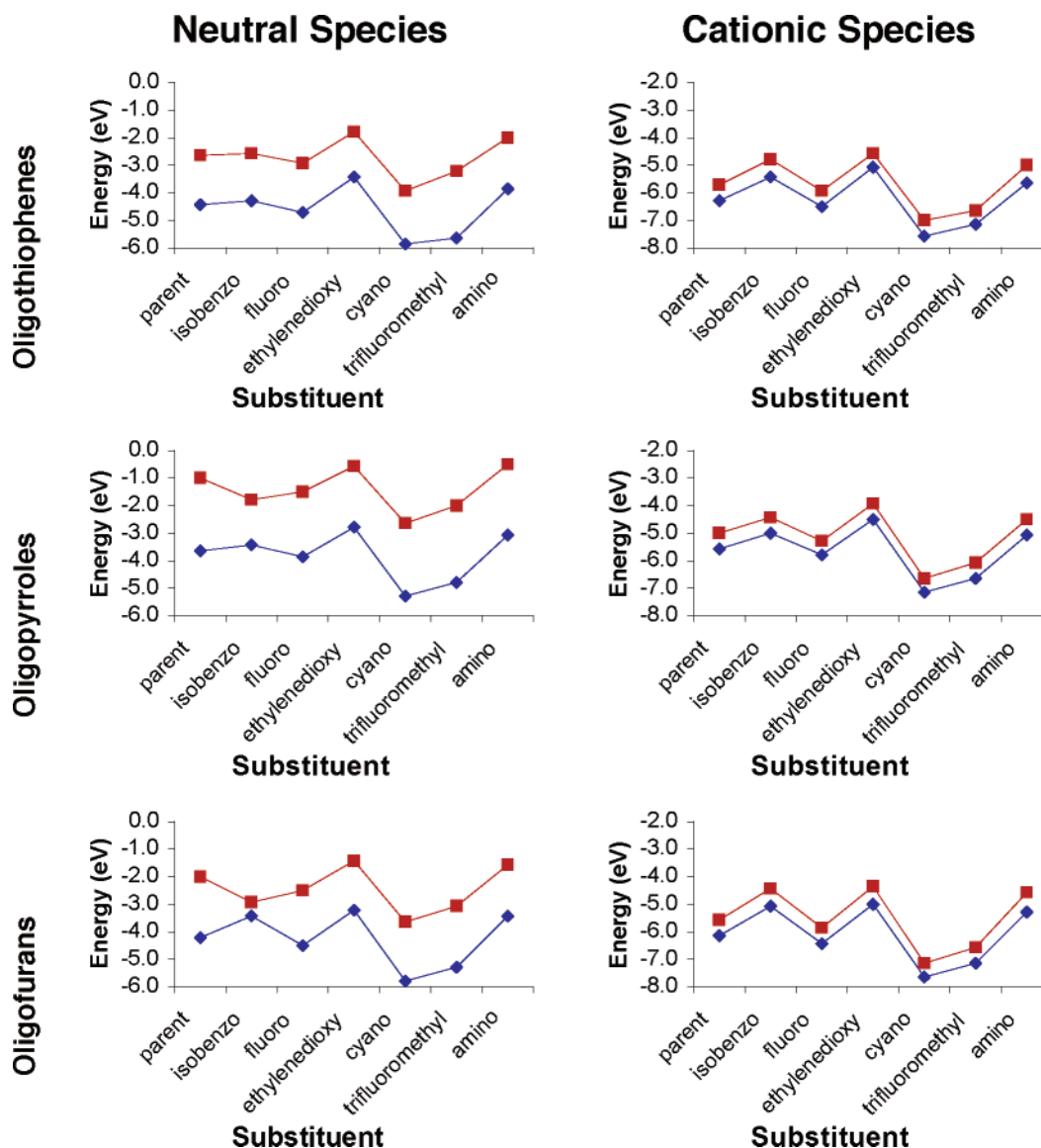


**Figure 7.** Comparison of the computed sensitivities of LUMO (■) and HOMO (◆) energies to various heteroatoms and substituents for neutral and cationic oligoheterocycles. The y-axis is shifted by 2 eV between the neutral and cationic species, as the cations have larger ionization potentials.



and charge, they have consequently been deleted from the analyses presented herein.

Before further considering the results of the linear models and the ANOVA results summarized in Tables 1 and 2, it is also important to consider whether the approximate  $1/N$  scaling of electronic structure as a function of oligomer length holds. Because the oligomers considered here are only 2–6 monomer units in length, the saturation effects observed at long oligomer lengths<sup>33</sup> should not contribute significantly. However, at the termini of oligomers, substituents may have minimal impact on inter-ring steric demands by extending away from the molecular core, whereas within the core of the molecule, encumbered groups such as trifluoromethyl may induce chain twisting (deviations from ring coplanarity) due to repulsive steric interactions with a neighboring heteroatom (e.g., sulfur); thus, the end group has reduced steric constraints. These “end group effects” should, of course, be more significant at short oligomer lengths such as in dimers or trimers and may be another source of deviations from  $1/N$  behavior. Tables S4 and S5 summarize the extrapolated electronic structures of each species obtained from the  $1/N$  relation and illustrate that with few exceptions, the  $1/N$  behavior provides an excellent fit ( $R^2 > 0.9$ ). The most notable exception comes in the HOMO and LUMO energies of series 2—a more planar conformation is preferred at shorter oligomer lengths than at longer ones—the effect can be observed in the HOMO trend of Figure S5(c).

The extrapolated orbital energies in Table S4 also reveal potential band crossing effects, particularly among the cationic species. In 10 of the 21 series, including families 1<sup>+</sup>, 6<sup>+</sup>, 8<sup>+</sup>, 10<sup>+</sup>, 12<sup>+</sup>, 13<sup>+</sup>, 15<sup>+</sup>, 17<sup>+</sup>, 19<sup>+</sup>, and 20<sup>+</sup>, the cations show extrapolated HOMO–1 level crossings with the HOMO level. In four series, 8, 13, 2<sup>+</sup>, and 16<sup>+</sup>, the extrapolated LUMO+1 level crosses the LUMO level. These effects potentially create a higher density of states near the band gap for the valence or conduction bands, respectively. The large number of cations having energetically proximate HOMO–1 and HOMO levels confirms the picture of the midgap states illustrated in Figure 4b—the singly occupied levels in the cation electronic structures tend to be very close to the doubly occupied level.

Although the intercepts in the  $1/N$  relation provide information on the extrapolated infinite polymers, the slopes provide information on the interaction between neighboring monomer units along the oligomer/polymer chain. If there were zero slope, then the oligomer or polymer electronic structure would be independent of chain length—a completely localized picture. On the other hand, a large slope indicates a system toward the limit of a far smaller band gap and a more delocalized C–C backbone. Furthermore, highly encumbered substituents could in principle twist the oligomer chain from planarity and alter the slope of, or even eliminate, the  $1/N$  scaling.

The above discussion indicates that the effects of oligomer length, substituent, heteroatom, and charge are by no means independent, and that second-order or higher interaction factors can be statistically significant. Indeed, although the “no-interaction” models comprised only the principal factors just discussed, e.g.

$$\Delta E = C_0 + C_1(1/N) + C_2(\text{heteroatom}) + C_3(\text{substituent}) + C_4(\text{charge}) \quad (4)$$

where  $C_0$ ,  $C_1$ ,  $C_2$ ,  $C_3$ , and  $C_4$  are coefficients of the multivariate fit, they predict the ZINDO/CIS and TDDFT excitation energies reasonably well ( $R^2 = 0.919$  and  $0.954$ , respectively; mean absolute errors =  $0.151$  eV and  $0.120$  eV, respectively), as

illustrated in Figure 5, although a large number of outliers are observed. (The results of these models are compiled in Table S3.) Interactions can also be discerned in plots of the HOMO and LUMO orbital energies in Figure 7, which show a clear difference in the response to substituents of neutral vs cationic species. Smaller differences are also observed in the response of the orbital energies to both heteroatom and heterocycle substituents, for example, in the close proximity of the HOMO and LUMO energies, in isobenzofurans. Such interactions are also evident in the ZINDO/CIS and TDDFT excitation energies, with a larger difference between the excitation energies of the neutrals and cations for isobenzopyrrole than for isobenzofuran or isobenzothiophene, as shown in Figure 8. For these reasons, such second-order and third-order interactions are found to be statistically significant by ANOVA, as shown in Table 1. Incorporation of these interactions into the statistical model significantly improves the accuracy of the model, as illustrated by the “complete models,” composed of the principal factors as well as second- and third-order interactions, of ZINDO/CIS and TDDFT excitation energies in Figure 5. These result in a formula

$$\begin{aligned} \Delta E = & C_0 + C_1(1/N) + C_2(\text{heteroatom}) + C_3(\text{substituent}) + \\ & C_4(\text{charge}) + C_5(1/N \cdot \text{heteroatom}) + C_6(1/N \cdot \text{substituent}) + \\ & C_7(1/N \cdot \text{charge}) + C_8(\text{heteroatom} \cdot \text{substituent}) + \\ & C_9(\text{heteroatom} \cdot \text{charge}) + C_{10}(\text{substituent} \cdot \text{charge}) + \dots \\ & (\text{third-order interactions}) \quad (5) \end{aligned}$$

where the various  $C_n$  parameters are fit by the multivariate regression and “ $\cdot$ ” is taken as a combination of two or more principal factors (e.g., substituent·cation might be inserted for substituent = isobenzene and charge = cation). In the case of categorical factors, such as heteroatom identity, substituent, and charge, the appropriate additive factor is looked up on the basis of the particular species, but for the continuous  $1/N$  factor representing oligomer length, the quantity  $1/N$  is multiplied by the appropriate additive factor. As an example, the fit from Table 2 for the TDDFT excitation energy of the neutral dimer of 11 would be

$$\begin{aligned} \Delta E \text{ (eV)} = & 1.21 + 5.31(1/2) + 0.47(\text{pyrrole}) - \\ & 0.07(\text{ethylenedioxy}) + 0 + 0.47(1/2 \cdot \text{pyrrole}) - 0.23 \times \\ & (1/2 \cdot \text{ethylenedioxy}) + 0 - 0.13(\text{pyrrole} \cdot \text{ethylenedioxy}) + \\ & 0 + 0 + \dots (\text{third-order interactions total: } +0.04) \quad (6) \end{aligned}$$

and the “charge” terms are all zero, because the categorical effects (heteroatom, substituent, and charge) are taken relative to the neutral oligothiophene parent 1. Thus, eq 6 predicts 4.18 eV, compared to the computed 4.27 eV. As mentioned above, such models are most useful for illustrating trends in the data as well as providing improved error analysis, rather than extrapolation of substituent effects or heterocycle identity for predicting properties directly.

**D. Effects of Length, Heteroatom, Heterocycle Substituent, and Interactions.** As outlined above and in Tables 1 and 2, substituent, heteroatom, length, and charge are clearly not completely independent in their effects on computed orbital and excitation energies. As another example, longer chain oligomers more readily stabilize a radical cation through increased delocalization, so that a strong interaction between the effects of oligomer length and charge can be assumed, even though these are varied independently in the sets of oligomers studied here. Hence, the intercepts and tabulated principal factors are



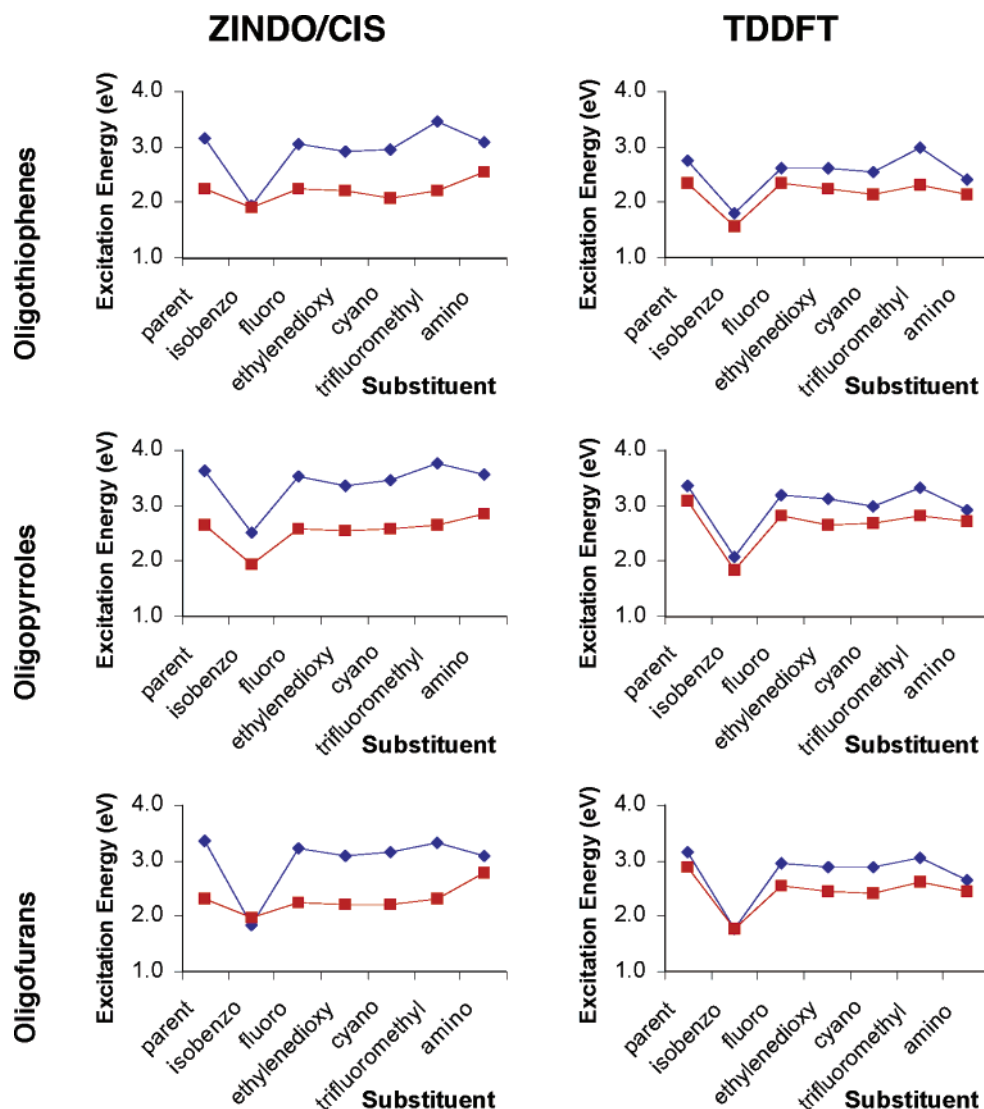


**Figure 8.** Comparison of the average (across oligomer length) computed ZINDO/CIS and TDDFT excitation energies of the various heteroatom series and substituent series for both neutral (◆) and cationic (■) oligoheterocycles.

not the only statistically significant effects, as indicated by the ANOVA results in Table 1 and by the nonzero coefficients in Table 2.

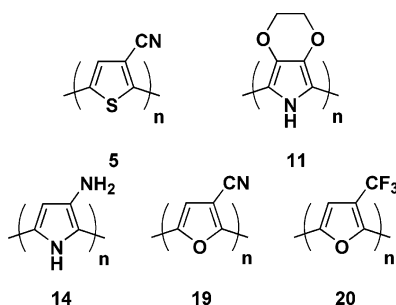
The principal factors observed here are the most obvious to explain in purely electronic terms. For example, the substituent effects, relative to the unsubstituted parent oligoheterocycles, show that electron-withdrawing substituents such as fluoro, cyano, and trifluoromethyl significantly lower the HOMO−1, HOMO, LUMO, and LUMO+1 levels, whereas isobenzo, ethylenedioxy, and amino all raise the orbital energies significantly, as seen in Table 2. Because such effects are not equal for the occupied and unoccupied states, the effects on excitation energies are more difficult to rationalize on a purely electron-donating or -withdrawing basis. In particular, isobenzo substitution appears to shrink the band gap via pushing up the HOMO−1 and HOMO levels more than the unoccupied levels, whereas trifluoromethyl substitution increases the band gap by pulling the occupied levels down by more than the unoccupied levels. The slightly smaller band gaps induced by ethylenedioxy or amino substitution, as predicted by TDDFT (Table 2), may derive from greater positive charge localization on carbon atoms 3 and 4 of the thiophene ring—the computed Mulliken charges on these atoms of series **2**, **4**, and **7** are +0.3–+0.5 vs

unsubstituted **1**, whereas **3**, **5**, and **6** are found to have smaller substituent charge effects.

The remainder of the substituents exert relatively small effects on excitation energies, particularly when compared with the second-order interactions between heteroatom and substituents. This implies that the effects of substituents on furans and pyrroles are often quite different than on thiophenes. As an example, the predicted effect of cyano substitution on the oligothiophene TDDFT excitation energies is negligible, but it is large in the case of furans and pyrroles, presumably because these heterocycles are more electron-rich (e.g., +0.30 and +0.86 eV for HOMO levels of oligofurans and oligopyrroles, respectively, and +0.57 and +1.60 eV for LUMO levels of oligofurans and oligopyrroles, respectively from Table 2, implying more facile oxidation involving HOMO levels and more difficult reduction involving LUMO levels). This trend also holds for the orbital energies—electron-withdrawing substituents such as cyano or trifluoromethyl have larger (negative) effects on the orbital energies of electron-rich furan or pyrrole rings, and electron-donating substituents have less (i.e., interaction effects <0) positive effects on the orbital energies of electron-rich furan or pyrrole rings. For example, an electron-donating substituent simply has a smaller effect on the electronic structure of an electron-rich heterocycle (e.g., an oligofuran) than on the

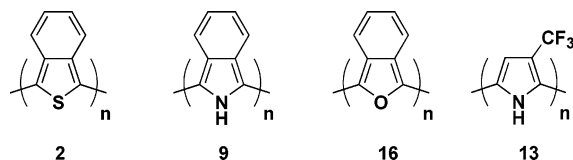
electron-poor oligothiophenes. Therefore, the actual electronic structure effect is *smaller* than would be expected by simply adding the furan and substituent effect—and so to correct this error, the second-order interaction is negative.

**E. Highs and Lows in Reduction, Oxidation, and Excitation Energies.** Beyond the aforementioned statistical trends, some instructive “highlights” are found at the extrema in the orbital energies and excitation energies. These may have noteworthy implications for materials design. Because the HOMO and LUMO energies correlate with ionization potential and electron affinity, low HOMO orbital energies and high LUMO energies are associated with species difficult to oxidize and reduce, respectively.<sup>43</sup> The lowest HOMO orbital energy for a neutral species is for the dimer of cyanothiophene oligomer **5** (−6.53 eV), nearly twice the computed ionization potential



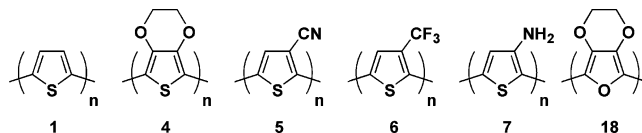
of the hexamer of ethylenedioxythiophene oligomer **11** (−3.27 eV), which has the highest lying HOMO energy. The range is also large for the HOMO energies of the cations, with the cyano-substituted structures still the most difficult to oxidize—the dimer of oligomer **19** has the lowest HOMO energy, with the dimer of oligomer **20** a close second (−11.43 and −11.24 eV, respectively) and the highest HOMO energy of a cation again belongs to the hexamer of oligomer **11** (−5.91 eV). The trifluoromethylfuran oligomers of **20** also have high LUMO energies, with the dimer computed to yield the second-highest LUMO (+0.44 eV, vs +0.49 eV for the dimer of **14**) and the hexamer yielding the highest LUMO among the cations (−4.98 eV). Conversely, oligomers of **5** have the lowest lying LUMO in the neutral state (−3.48 eV for the hexamer) and the second-lowest LUMO for the cation oligomers (−9.52 eV for the dimer, vs −9.69 eV for the dimer of **19**). In short, ethylenedioxy and amino substituents are strong electron-donating groups and strongly push up HOMO and LUMO levels, whereas the cyano group is the strongest electron-withdrawing substituent found here. Such trends have significant implications for the design of n-type or p-type organic thin-film transistor active components and redox polymers.<sup>44</sup>

In terms of computed excitation energies, the smallest belong to the isobenzofuran family with the lowest TDDFT excitation energy computed for the neutral oligomers (hexamer) of **16**, 1.29 eV,

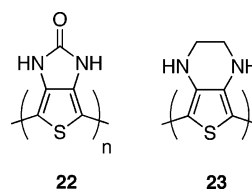


as well as cationic oligomers (hexamer) of **2**, 1.18 eV, vs 1.33 eV for the hexamer of **16**, as well as the lowest ZINDO/CIS excitation energies for neutral oligomers (hexamer) of **16**, 1.24 eV, and cationic oligomers (hexamer) of **9**, 1.48 eV, vs 1.52 eV for the hexamer of **2**. Interestingly, the highest computed excitation energies belong to unsubstituted oligopyrrole **8**,

computed to have the highest TDDFT excitation energy in both the neutral and cationic dimers (4.54 and 4.25 eV, respectively), the second-highest ZINDO/CIS excitation energy for the neutral dimer (4.46 eV vs 4.53 eV for the dimer of **13**) and the highest ZINDO/CIS excitation energy for the dimer monocation (4.72 eV). Beyond predicting the smallest excitation energies, however, TDDFT and ZINDO/CIS methods also predict that several of the oligomers should have high optical transparency, with the most intense excitations in the near-IR (i.e., <1.7 eV for the primary excitations and few strong additional higher energy transitions). These oligoheterocycles include the monocation hexamers of **4**, **5**, and **7** and various oligomers (both neutral and cationic) of **2**, **9**, and **16**, as computed by TDDFT, and hexamers of **1**, **4**, **5**, **6**, and **18**, and again various oligomers of



**2**, **9**, and **16**, as computed by ZINDO/CIS. Thus, from these results, PEDOT (modeled by oligomers of **4** or by the pyrrole analogue **11**) is predicted *not* to be the only potential conductive polymer that is transparent in the visible range as sometimes assumed.<sup>14</sup> In particular, we suggest oligomers **22** and **23** as



potential transparent conducting polymers, extending the trends in smaller band gaps observed in the ethylenedioxy- and amino-substituted oligomers discussed above. The TDDFT-computed band gaps of **22** and **23** are equal to or lower than the corresponding ethylenedioxy-substituted oligothiophenes (**4**) (extrapolated 1/N polymer band gaps of 1.63, 1.62, and 1.7 eV for **22**, **23**, and **4**, respectively) and also show no strong higher energy optical excitations. Because oligomer **22** should participate in interchain hydrogen-bonding, we suggest that it may self-assemble into well-ordered polymer networks for higher conductivity.

**F. Relation Between Neutral and Cationic Oligomer Band Gaps.** Both the ZINDO/CIS and TDDFT comparisons reveal roughly linear correlations between the excitation energies of the neutral and the corresponding cationic species, as shown in Figure 9:

$$E_{\text{cation}} = 0.114 \text{ eV} + 0.717E_{\text{neutral}} \quad (7a)$$

$$E_{\text{cation}} = 0.046 \text{ eV} + 0.861E_{\text{neutral}} \quad (7b)$$

for ZINDO/CIS (eq 7a) and TDDFT (eq 7b) energies, respectively. In general, a net red shift is observed for the cationic vs neutral species, resulting in approximately 70–85% of the band gap energies of the corresponding neutral species for the higher energy transition of the two radical cation excitations, whereas the weaker, lower energy transition results in ~40% of the band gap of the neutral (Figure S2). For both computational methods, small but finite y-intercepts are found, indicating that a zero band gap neutral molecule would be predicted to have a finite, positive gap as a cation. In fact, the “break-even” points, where a neutral species and cation would have the same band gap,

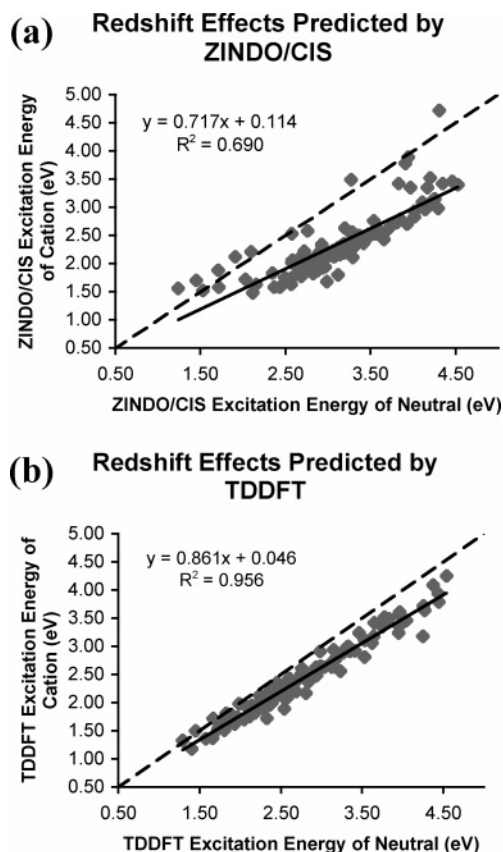


**Figure 9.** Comparison of neutral and cationic oligoheterocycle excitation energies computed by (a) ZINDO/CIS and (b) TDDFT. Solid lines indicate the regression trend with fits indicated, and the dotted lines indicate a 1:1 correlation, where the excitation energies for both species are equal. Note that for both computational formalisms, several oligomers have cations with computed band gap energies larger than those of the neutral compounds (i.e., blue shifted).

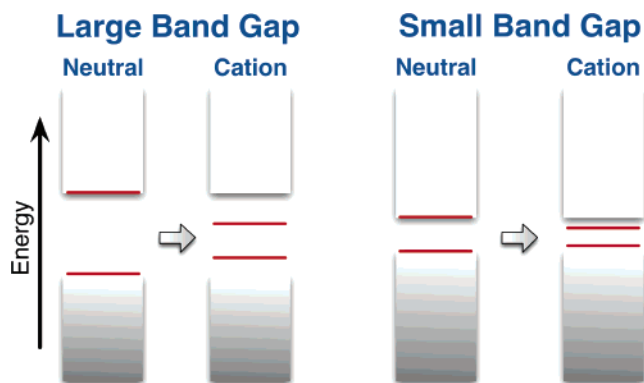


**Figure 10.** Schematic of the fixed band approximation, assuming that upon oxidation from neutral to monocation, the positions of the valence and conduction band edges do not change relative energetics. As illustrated, for small band gap compounds, the electronic structure of the small band gap monocations (including midgap states) are very similar to that of the neutral oligomers, particularly when compared to the electronic structure changes in large band gap oligomers.

predicted by the linear correlations from both computational methods, are very similar—between 0.3 and 0.5 eV. The greatest red shift in TDDFT excitation energy from neutral to monocation is for the dimer of series **17** (−1.07 eV), whereas the dimer of series **5** is second (−0.72 eV), and the largest blue shift is computed for the tetramer of series **16** (+0.05 eV).

The differences in C–C bond lengths between neutral and radical cation oligomers are shown in Figure S6 for tetrafulan

(oligomer series **15**) and tetraisobenzofuran oligomers (oligomer series **16**). Compared to the parent neutral and cation oligofurans, the neutral and cation tetramer species of **16** are computed to have far smaller dispersions in the C–C bond lengths—26.6% smaller overall. The differences in computed Mulliken charges are 28.7% smaller overall for oligomer **16** than for **15**, because some of the positive charge is delocalized onto the fused isobenzofuran substituents. The overall conclusion is that polaronic distortion is largely suppressed in oligomer class **16**, due to increased delocalization, and the neutral and cationic forms have very similar electronic structures, much like analogous oligothiophenes **2** and **2**<sup>+</sup> in Figures S5c,d, respectively. Consequently, the excitation energies in series **16** are very similar in the corresponding neutral and cationic oligomers. However, because the cations consistently have a greater contribution from the doubly occupied HOMO−1 level than do the neutral molecules, the result is an increased band gap in the cationic vs the neutral species.

This “blue-shift” effect can be rationalized on the basis of a fixed-band approximation. If the species has a small band gap in the neutral state, then the midgap levels are constrained energetically, and the orbital energetics of the cation will be very similar to those of the neutral molecule. Because Figure 9 shows that both ZINDO/CIS and TDDFT formalisms predict this linear trend, it is clear that this is a statistically significant general rule, and not specific to the isobenzofuran substituent. Other substituents show small red shifts, and the smaller the predicted band gap in the neutral species, the closer to the break-even point overall. Because experimental measurements suggest that certain conjugated heterocyclic polymers have band gaps in the range of 0.7–0.8 eV<sup>40</sup> and even ~0.5 eV,<sup>45</sup> the use of the fixed band approximation and understanding this blue-shift effect in cationic states should aid the design of small band gap materials and have significant implications for development of novel electrochromic materials.

#### IV. Conclusions

The present systematic, multidimensional computational study across a wide range of oligoheterocycles, substituents, and oligomer chain lengths shows that, contrary to the conventional picture, midgap states lie much closer to doubly occupied valence states than to the unoccupied states, and that the position of these states varies considerably, due to an interplay of heteroatom, heterocycle substituent, and conjugation length effects. Extrapolation toward the infinite polymer electronic structure via the conventional 1/*N* relation demonstrates that many oligoheterocyclic cations exhibit band crossings of the singly occupied and doubly occupied levels, further indicating a high density of states near the valence band edge in the p-doped species. Furthermore, interpreting the results using statistical models indicates that simplistic structural metrics such as carbon–carbon backbone bond length alternation and interring dihedral angle are not particularly effective at predicting the overall electronic structure (particularly excitation energetics) of these oligoheterocycles. Comparison of substituent and heteroatom effects across the set indicates that very significant interaction effects exist, which are in some cases not straightforward to rationalize, particularly in how they affect computed excitation energies. Consequently, although heteroatom and substituent effects may adhere to systematic qualitative “rules of thumb,” the subtle interplay between the effects illustrates that modeling particular individual systems is far more reliable than attempting to sum tabulated heteroatom and substituent effects.



Taking into account the structural variations of oligomers studied here, it is possible to identify several candidate structures as potential transparent conductive polymers, and others are computed to show limiting values of oxidation/reduction potentials, small and large band gaps for both neutral and monocation species.

It is also clear from the present results that relatively simple and straightforward predictors of ZINDO/CIS and TDDFT excitation energies can be based on the frontier orbital energies computed by DFT, because in these particular oligoheterocycles, the extent of orbital mixing appears relatively consistent. Furthermore, a linear relation exists, eq 7, between the computed excitation energies of the neutral molecule and those of the corresponding monocation species with the latter generally exhibiting reduced excitation energies. This relation confirms the effectiveness of the "fixed band" approximation as well as an increase in effective band gap for p-doped small band gap materials (i.e., 0.3–0.5 eV) because the midgap states do not shift significantly.

**Acknowledgment.** We thank the NSF/MRSEC program through the Northwestern University MRSEC (NSF DMR-0076097), the ONR (N00014-02-1-0909), and the NASA Institute for Nanoelectronics and Computing (Award NCC 2-3163) for support. We are grateful to Prof. Jeff Reimers for his CNDO program for ZINDO/CIS calculations.

**Supporting Information Available:** Table and figure comparing computed ZINDO/CIS and TDDFT excitation energies with experimental radical cation data<sup>8,18</sup> for series **1** and **8**. Tables of third-order interaction effects and a simplified model for orbital energies and excitation energies (ZINDO/CIS, TDDFT). This material is available free of charge via the Internet at <http://pubs.acs.org>.

## References and Notes

- (1) Shirakawa, H.; Louis, E. J.; MacDiarmid, A. G.; Chiang, C. K.; Heeger, A. J. *J. Chem. Soc., Chem. Commun.* **1977**, 578. Shirakawa, H. *Angew. Chem., Int. Ed. Engl.* **2001**, *40*, 2575. Heeger, A. J. *Angew. Chem., Int. Ed. Engl.* **2001**, *40*, 2591. MacDiarmid, A. G. *Angew. Chem., Int. Ed. Engl.* **2001**, *40*, 2581.
- (2) Marks, T. J. *J. Coat Technol.* **1976**, *48*, 53.
- (3) Vardeny, Z.; Ehrenfreund, E.; Brafman, O.; Nowak, M.; Schaffer, H.; Heeger, A. J.; Wudl, F. *Phys. Rev. Lett.* **1986**, *56*, 671. Kivelson, S.; Heeger, A. J. *Synth. Met.* **1987**, *17*, 183.
- (4) Heeger, A. J.; Kivelson, S.; Schrieffer, J. R.; Su, W. P. *Rev. Mod. Phys.* **1988**, *60*, 781.
- (5) Gao, Y.; Liu, C. G.; Jiang, Y. S. *J. Phys. Chem. A* **2002**, *106*, 5380. Brocks, G. *Synth. Met.* **1999**, *102*, 914. Paasch, G.; Nguyen, P. H.; Fisher, A. J. *Chem. Phys.* **1998**, *227*, 219. Irle, S.; Lischka, H. *J. Chem. Phys.* **1997**, *107*, 3021. Casado, J.; Ramirez, F. J.; Hotta, S.; Navarrete, J. T. L.; Hernandez, V. *Synth. Met.* **1997**, *84*, 571. Brédas, J. L.; Beljonne, D.; Cornil, J.; dosSantos, D. A.; Shuai, Z. *Philos. Trans. R. Soc. London, A* **1997**, *355*, 735. Tol, A. J. W. *Chem. Phys.* **1996**, *208*, 73. Yokonuma, N.; Furukawa, Y.; Tasumi, M.; Kuroda, M.; Nakayama, J. *Chem. Phys. Lett.* **1996**, *255*, 431. Irle, S.; Lischka, H. *THEOCHEM-J. Mol. Struct.* **1996**, *364*, 15. Waragai, K.; Akimichi, H.; Hotta, S.; Kano, H.; Sakaki, H. *Phys. Rev. B* **1995**, *52*, 1786. Miller, L. L.; Yu, Y.; Gunic, E.; Duan, R. *Adv. Mater.* **1995**, *7*, 547. Poplawski, J.; Ehrenfreund, E.; Cornil, J.; Brédas, J. L.; Pugh, R.; Ibrahim, M.; Frank, A. J. *Mol. Cryst. Liq. Cryst. Sci. Technol. A* **1994**, *256*, 407. Xie, S. J.; Mei, L. M.; Lin, D. L. *Phys. Rev. B* **1994**, *50*, 13364. Diers, J. R.; Dearmond, M. K.; Guay, J.; Diaz, A.; Wu, R. L.; Schumm, J. S.; Tour, J. M. *Chem. Mater.* **1994**, *6*, 327. Soos, Z. G.; Galvao, D. S. *J. Phys. Chem.* **1994**, *98*, 1029. Steinmuller, D.; Ramsey, M. G.; Netzer, F. P. *Phys. Rev. B* **1993**, *47*, 13323. Onoda, M.; Nakayama, H.; Morita, S.; Yoshino, K. *J. Appl. Phys.* **1993**, *73*, 2859. Deussen, M.; Bassler, H. *Synth. Met.* **1993**, *54*, 49. Bussac, M. N.; Zuppiroli, L. *Phys. Rev. B* **1993**, *47*, 5493. Onoda, M.; Manda, Y.; Morita, S.; Yoshino, K. *Jpn. J. Appl. Phys. Part 1* **1992**, *31*, 2265. Boman, M.; Stafström, S. *Phys. Rev. B* **1992**, *46*, 4551. Deussen, M.; Bassler, H. *Chem. Phys.* **1992**, *164*, 247. Springborg, M. J. *Phys.: Condens. Matter* **1992**, *4*, 101. Conwell, E. M.; Mizes, H. A.; Choi, H. Y. *Synth. Met.* **1991**, *43*, 3675. Stafström, S.; Brédas, J. L. *Mol. Cryst. Liq. Cryst.* **1988**, *160*, 405. Bertho, D.; Jouanin, C. *Phys. Rev. B* **1987**, *35*, 626.
- (6) Irle, S.; Lischka, H. *J. Chem. Phys.* **1995**, *103*, 1508. Furukawa, Y. *Synth. Met.* **1995**, *69*, 629. Faied, K.; Leclerc, M.; Nguyen, M.; Diaz, A. *Macromolecules* **1995**, *28*, 284. Furukawa, Y.; Yokonuma, N.; Tasumi, M.; Kuroda, M.; Nakayama, J. *Mol. Cryst. Liq. Cryst. Sci. Technol. A* **1994**, *256*, 113. Fichou, D.; Horowitz, G.; Garnier, F. *Synth. Met.* **1990**, *39*, 125.
- (7) Gustafsson, J. C.; Pei, Q.; Inganäs, O. *Solid State Commun.* **1993**, *87*, 265.
- (8) Fichou, D.; Horowitz, G.; Xu, B.; Garnier, F. *Synth. Met.* **1990**, *39*, 243.
- (9) Springborg, M. *Synth. Met.* **1997**, *85*, 1037. Furukawa, Y.; Sakamoto, A.; Ohta, H.; Tasumi, M. *Synth. Met.* **1992**, *49*, 335. Bally, T.; Roth, K.; Tang, W.; Schrock, R. R.; Knoll, K.; Park, L. Y. *J. Am. Chem. Soc.* **1992**, *114*, 2440. Tabor, S.; Stafström, S. *Phys. Rev. B* **1991**, *44*, 12737. Stafström, S.; Brédas, J. L. *Synth. Met.* **1989**, *28*, D477. Voit, J. *Synth. Met.* **1989**, *28*, D495. Stafström, S.; Brédas, J. L. *Phys. Rev. B* **1988**, *38*, 4180. Jeyadev, S.; Conwell, E. M. *Phys. Rev. B* **1987**, *35*, 6253. Glick, A. J.; Bryant, G. W. *Phys. Rev. B* **1986**, *34*, 943. Conwell, E. M. *Phys. Rev. B* **1986**, *33*, 2465. Yamabe, T.; Tanaka, K.; Koike, T.; Ueda, M. *Mol. Cryst. Liq. Cryst.* **1985**, *117*, 185. Conwell, E. M. *Mol. Cryst. Liq. Cryst.* **1985**, *117*, 155. Dos Santos, M. C.; De Melo, C. P.; Brandi, H. S. *Solid State Commun.* **1984**, *52*, 99. Friend, R. H. *NATO ASI Ser., Ser. C* **1984**, *130*, 625. Onodera, Y. *Phys. Rev. B* **1984**, *30*, 775. Brédas, J. L.; Themans, B.; Andre, J. M.; Chance, R. R.; Silbey, R. *Synth. Met.* **1984**, *9*, 265. Zannoni, G.; Zerbi, G. *Solid State Commun.* **1984**, *50*, 55. Boudreaux, D. S.; Chance, R. R.; Brédas, J. L.; Silbey, R. *Phys. Rev. B* **1983**, *28*, 6927. Bishop, A. R.; Campbell, D. K.; Fesser, K. J. *Phys. Colloque* **1983**, *423*. Sano, T.; I'Haya, Y. J. *J. Chem. Phys.* **1983**, *79*, 2060. Fesser, K.; Bishop, A. R.; Campbell, D. K. *Phys. Rev. B* **1983**, *27*, 4804. Suhai, S. *Phys. Rev. B* **1983**, *27*, 3506. Campbell, D. K.; Bishop, A. R.; Fesser, K. *Phys. Rev. B* **1982**, *26*, 6862. Brédas, J. L.; Chance, R. R.; Silbey, R. *Phys. Rev. B* **1982**, *26*, 5843. Brédas, J. L.; Chance, R. R.; Silbey, R. *Mol. Cryst. Liq. Cryst.* **1981**, *77*, 319. Bishop, A. R. *Solid State Commun.* **1980**, *33*, 955.
- (10) Chaudhury, P.; Bhattacharyya, S. P. *Int. J. Quantum Chem.* **2003**, *91*, 663. Moro, G.; Scalmani, G.; Cosentino, U.; Pitea, D. *Synth. Met.* **2000**, *108*, 165. Fagerström, J.; Stafström, S. *Phys. Rev. B* **1996**, *54*, 13713. Giri, D.; Kundu, K. *Phys. Rev. B* **1996**, *53*, 4340. Boman, M.; Stafström, S. *Synth. Met.* **1993**, *57*, 4614. Hill, M. G.; Mann, K. R.; Miller, L. L.; Penneau, J. F. *J. Am. Chem. Soc.* **1992**, *114*, 2728. Fichou, D.; Xu, B.; Horowitz, G.; Garnier, F. *Synth. Met.* **1991**, *41*, 463. Springborg, M. *Synth. Met.* **1991**, *43*, 3541. Stafström, S.; Brédas, J. L. *Mol. Cryst. Liq. Cryst.* **1988**, *160*, 405. Brédas, J. L.; Wudl, F.; Heeger, A. J. *Solid State Commun.* **1987**, *63*, 577. Dos Santos, M. C.; De Melo, C. P.; Brandi, H. S. *Int. J. Quantum Chem.* **1986**, *30*, 109. Hattori, T.; Hayes, W.; Wong, K.; Kaneto, K.; Yoshino, K. J. *Phys. C: Solid State Phys.* **1984**, *17*, L803. Kaneto, K.; Kohno, Y.; Yoshino, K. *Solid State Commun.* **1984**, *51*, 267. Chung, T. C.; Kaufman, J. H.; Heeger, A. J.; Wudl, F. *Phys. Rev. B* **1984**, *30*, 702.
- (11) Brédas, J. L.; Themans, B.; Fripiat, J. G.; Andre, J. M.; Chance, R. R. *Phys. Rev. B* **1984**, *29*, 6761.
- (12) Appel, G.; Bohme, O.; Mikalo, R.; Schmeisser, D. *Chem. Phys. Lett.* **1999**, *313*, 411. Shimoi, Y.; Abe, S. *Phys. Rev. B* **1994**, *50*, 14781. Hu, Y.; Yang, R.; Evans, D. F.; Weaver, J. H. *Phys. Rev. B* **1991**, *44*, 13660. Batz, P.; Schmeisser, D.; Goepel, W. *Phys. Rev. B* **1991**, *43*, 9178. Reghu, M.; Subramanyam, S. V.; Chatterjee, S. *Phys. Rev. B* **1991**, *43*, 4236. Zotti, G.; Schiavon, G. *Chem. Mater.* **1991**, *3*, 62. Devreux, F.; Genoud, F.; Nechtschein, M.; Villeret, B. *Springer Ser. Solid-State Sci.* **1987**, *76*, 270. Genoud, F.; Guglielmi, M.; Nechtschein, M.; Genies, E.; Salmon, M. *Phys. Rev. Lett.* **1985**, *55*, 118. Kaufman, J. H.; Colaneri, N.; Scott, J. C.; Street, G. B. *Phys. Rev. Lett.* **1984**, *53*, 1005. Scott, J. C.; Pfluger, P.; Krounbi, M. T.; Street, G. B. *Phys. Rev. B* **1983**, *28*, 1240. Brédas, J. L.; Themans, B.; Andre, J. M. *Phys. Rev. B* **1983**, *27*, 7827.
- (13) Gaupp, C. L.; Zong, K.; Schottland, P.; Thompson, B. C.; Thomas, C. A.; Reynolds, J. R. *Macromolecules* **2000**, *33*, 1132. Welsh, D. M.; Kumar, A.; Meijer, E. W.; Reynolds, J. R. *Adv. Mater.* **1999**, *11*, 1379. Sapp, S. A.; Sotzing, G. A.; Reynolds, J. R. *Chem. Mater.* **1998**, *10*, 2101. Mortimer, R. J. *J. Chem. Soc. Rev.* **1997**, *26*, 147. Pei, Q.; Zuccarello, G.; Ahlskog, M.; Inganäs, O. *Polymer* **1994**, *35*, 1347.
- (14) Groenendaal, L.; Jonas, F.; Freitag, D.; Pielartzik, H.; Reynolds, J. R. *Adv. Mater.* **2000**, *12*, 481.
- (15) Hutchison, G. R.; Ratner, M. A.; Marks, T. J. *J. Phys. Chem. A* **2002**, *106*, 10596.
- (16) Hirata, S.; Lee, T. J.; Head-Gordon, M. *J. Chem. Phys.* **1999**, *111*, 8904. Halasinski, T. M.; Weisman, J. L.; Ruiterkamp, R.; Lee, T. J.; Salama, F.; Head-Gordon, M. *J. Phys. Chem. A* **2003**, *107*, 3660. Grozema, F. C.; Van Duijnen, P. T.; Siebbeles, L. D. A.; Goossens, A.; De Leeuw, S. W. *J. Phys. Chem. B* **2004**, *108*, 16139.
- (17) Casado, J.; Miller, L. L.; Mann, K. R.; Pappenfus, T. M.; Higuchi, H.; Orti, E.; Milian, B.; Pou-Amerigo, R.; Hernandez, V.; Lopez Navarrete, J. T. *J. Am. Chem. Soc.* **2002**, *124*, 12380. Pappenfus, T. M.; Raff, J. D.; Hukkanen, E. J.; Burney, J. R.; Casado, J.; Drew, S. M.; Miller, L. L.; Mann, K. R. *J. Org. Chem.* **2002**, *67*, 6015. Apperloo, J. J.; Groenendaal,



- L. B.; Verheyen, H.; Jayakannan, M.; Janssen, R. A. J.; Dkhissi, A.; Beljonne, D.; Lazzaroni, R.; Brédas, J.-L. *Chem.—Eur. J.* **2002**, *8*, 2384.
- Apperloo, J. J.; Janssen, R. A. J.; Malenfant, P. R. L.; Groenendaal, L.; Fréchet, J. M. J. *J. Am. Chem. Soc.* **2000**, *122*, 7042.
- Inoue, S.; Nakanishi, H.; Takimiya, K.; Aso, Y.; Otsubo, T. *Synth. Met.* **1997**, *84*, 341.
- Yu, Y.; Gunic, E.; Zinger, B.; Miller, L. L. *J. Am. Chem. Soc.* **1996**, *118*, 1013.
- Hotta, S.; Waragai, K. *J. Phys. Chem.* **1993**, *97*, 7427.
- Bäuerle, P.; Segelbacher, U.; Maier, A.; Mehring, M. *J. Am. Chem. Soc.* **1993**, *115*, 10217.
- (18) (a) Van Haare, J. A. E. H.; Havinga, E. E.; Van Dongen, J. L. J.; Janssen, R. A. J.; Cornil, J.; Brédas, J.-L. *Chem.—Eur. J.* **1998**, *4*, 1509.
- (b) Martina, S. Synthesis and Properties of Oligo(2,5-Pyrrole)s. Ph.D. Dissertation, Johannes-Gutenberg-Universität, Mainz, Germany, 1992.
- (19) Abboto, A.; Bradamante, S.; Pagani, G. A. *J. Org. Chem.* **1993**, *58*, 444.
- Hammett, L. P. *J. Am. Chem. Soc.* **1937**, *59*, 96.
- (20) Kong, J.; White, C. A.; Krylov, A. I.; Sherrill, C. D.; Adamson, R. D.; Furlani, T. R.; Lee, M. S.; Lee, A. M.; Gwaltney, S. R.; Adams, T. R.; Ochsenfeld, C.; Gilbert, A. T. B.; Kedziora, G. S.; Rassolov, V. A.; Maurice, D. R.; Nair, N.; Shao, Y.; Besley, N. A.; Maslen, P. E.; Dombroski, J. P.; Dachselt, H.; Zhang, W. M.; Korambath, P. P.; Baker, J.; Byrd, E. F. C.; Van Voorhis, T.; Oumi, M.; Hirata, S.; Hsu, C. P.; Ishikawa, N.; Florian, J.; Warshel, A.; Johnson, B. G.; Gill, P. M. W.; Head-Gordon, M.; Pople, J. A. *J. Comput. Chem.* **2000**, *21*, 1532.
- (21) Becke, A. D. *J. Chem. Phys.* **1993**, *98*, 5648.
- Lee, C.; Yang, W.; Parr, R. G. *Phys. Rev. B* **1988**, *37*, 785.
- (22) We use HOMO, LUMO, etc. as convenient shorthands, because electronic states, not one-electron levels, are actually measured experimentally.
- (23) Cornil, J.; Beljonne, D.; Brédas, J. L. *J. Chem. Phys.* **1995**, *103*, 842.
- (24) Perdew, J. P.; Levy, M. *Phys. Rev. B* **1997**, *56*, 16021.
- Seidl, A.; Gorling, A.; Vogl, P.; Majewski, J. A.; Levy, M. *Phys. Rev. B* **1996**, *53*, 3764.
- Levy, M. *Phys. Rev. A* **1995**, *52*, R4313.
- Godby, R. W.; Schluter, M.; Sham, L. J. *Phys. Rev. B* **1988**, *37*, 10159.
- (25) Zhan, C. G.; Nichols, J. A.; Dixon, D. A. *J. Phys. Chem. A* **2003**, *107*, 4184.
- (26) Rienstra-Kiracofe, J. C.; Tschumper, G. S.; Schaefer, H. F.; Nandi, S.; Ellison, G. B. *Chem. Rev.* **2002**, *102*, 231.
- Curtiss, L. A.; Redfern, P. C.; Raghavachari, K.; Pople, J. A. *J. Chem. Phys.* **1998**, *109*, 42.
- (27) Rienstra-Kiracofe, J. C.; Barden, C. J.; Brown, S. T.; Schaefer, H. F. *J. Phys. Chem. A* **2001**, *105*, 524.
- de Oliveira, G.; Martin, J. M. L.; de Proft, F.; Geerlings, P. *Phys. Rev. A* **1999**, *60*, 1034.
- DeProft, F.; Geerlings, P. *J. Chem. Phys.* **1997**, *106*, 3270.
- (28) Muscat, J.; Wander, A.; Harrison, N. M. *Chem. Phys. Lett.* **2001**, *342*, 397.
- (29) Hutchison, G. R. Theoretical Studies of Optics and Charge Transport in Organic Conducting Oligomers and Polymers: Rational Design of Improved Transparent and Conducting Polymers. Ph.D. Dissertation, Northwestern University, Evanston, Illinois, 2004.
- (30) Ridley, J.; Zerner, M. *Theor. Chim. Acta* **1973**, *32*, 111.
- (31) Reimers, J. R., CNDO/S Program, personal communication.
- (32) Ihaka, R.; Gentleman, R. *J. Comput. Graph. Statist.* **1996**, *5*, 299.
- (33) Hutchison, G. R.; Zhao, Y. J.; Delley, B.; Freeman, A. J.; Ratner, M. A.; Marks, T. J. *Phys. Rev. B* **2003**, *68*, 035204.
- (34) de Melo, J. S.; Silva, L. M.; Arnaut, L. G.; Becker, R. S. *J. Chem. Phys.* **1999**, *111*, 5427.
- Taubmann, G. *J. Chem. Educ.* **1992**, *69*, 96.
- (35) Kuhn, H. *J. Chem. Phys.* **1949**, *17*, 1198.
- (36) Parac, M.; Grimme, S. *Chem. Phys.* **2003**, *292*, 11.
- Parac, M.; Grimme, S. *J. Phys. Chem. A* **2002**, *106*, 6844.
- Grimme, S.; Parac, M. *ChemPhysChem* **2003**, *4*, 292.
- Hirata, S.; Zhan, C.-G.; Apra, E.; Windus, T. L.; Dixon, D. A. *J. Phys. Chem. A* **2003**, *107*, 10154.
- Tawada, Y.; Tsuneda, T.; Yanagisawa, S.; Yanai, T.; Hirao, K. *J. Chem. Phys.* **2004**, *120*, 8425.
- Dreuw, A.; Head-Gordon, M. *J. Am. Chem. Soc.* **2004**, *126*, 4007.
- Vasiliev, I.; Martin, R. M. *Phys. Rev. A* **2004**, *69*, 052508/1.
- Cai, Z. L.; Sendt, K.; Reimers, J. R. *J. Chem. Phys.* **2002**, *117*, 5543.
- Grozema, F. C.; Telesca, R.; Jonkman, H. T.; Siebbeles, L. D. A.; Snijders, J. G. *J. Chem. Phys.* **2001**, *115*, 10014.
- (37) Springborg, M.; Schmidt, K.; Meider, H.; De Maria, L. Theoretical Studies of Electronic Properties of Conjugated Polymers. In *Organic Electronic Materials: Conjugated Polymers and Low Molecular Weight Organic Solids*; Farchioni, R.; Grosso, G., Eds.; Springer: Berlin, 2001; Vol. 41; p 39.
- (38) Springborg, M. *Solid State Commun.* **1994**, *89*, 665.
- (39) Shimizu, Y.; Shen, Z.; Ito, S.; Uno, H.; Daube, J.; Ono, N. *Tetrahedron Lett.* **2002**, *43*, 8485.
- Cornil, J.; Vanderdonckt, S.; Lazzaroni, R.; dos Santos, D. A.; Thys, G.; Geise, H. J.; Yu, L. M.; Szablewski, M.; Bloor, D.; Logdlund, M.; Salaneck, W. R.; Gruhn, N. E.; Lichtenberger, D. L.; Lee, P. A.; Armstrong, N. R.; Brédas, J. L. *Chem. Mater.* **1999**, *11*, 2436.
- Roncali, J. *Chem. Rev.* **1997**, *97*, 173.
- Zerbi, G.; Magnoni, M. C.; Hoogmartens, I.; Kiebooms, R.; Carleer, R.; Vanderzande, D.; Gelan, J. *Adv. Mater.* **1995**, *7*, 1027.
- Kiebooms, R.; Hoogmartens, I.; Adriaenssens, P.; Vanderzande, D.; Gelan, J. *Macromolecules* **1995**, *28*, 4961.
- Quattrocchi, C.; Lazzaroni, R.; Brédas, J. L.; Kiebooms, R.; Vanderzande, D.; Gelan, J.; Vanmeervelt, L. *J. Phys. Chem.* **1995**, *99*, 3932.
- Hoogmartens, I.; Adriaenssens, P.; Vanderzande, D.; Gelan, J.; Quattrocchi, C.; Lazzaroni, R.; Brédas, J. L. *Macromolecules* **1992**, *25*, 7347.
- Karpfen, A.; Kertesz, M. *J. Phys. Chem.* **1991**, *95*, 7680.
- Brédas, J. L.; Heeger, A. J.; Wudl, F. *J. Chem. Phys.* **1986**, *85*, 4673.
- Kobayashi, M.; Colaneri, N.; Boysel, M.; Wudl, F.; Heeger, A. J. *J. Chem. Phys.* **1985**, *82*, 5717.
- Wudl, F.; Kobayashi, M.; Heeger, A. J. *J. Org. Chem.* **1984**, *49*, 3382.
- (40) Pomerantz, M. Low Band Gap Conducting Polymers. In *Handbook of Conducting Polymers*, 2nd ed.; Skotheim, T. A.; Elsenbaumer, R. L.; Reynolds, J. R., Eds.; Marcel Dekker: New York, **1998**; p 277.
- (41) Lee, Y. S.; Kertesz, M. *J. Chem. Phys.* **1988**, *88*, 2609.
- (42) Choi, C. H.; Kertesz, M. *J. Chem. Phys.* **1998**, *108*, 6681.
- Ho Choi, C.; Kertesz, M.; Karpfen, A. *J. Chem. Phys.* **1997**, *107*, 6712.
- Gorman, C. B.; Marder, S. R. *Chem. Mater.* **1995**, *7*, 215.
- Meyers, F.; Marder, S. R.; Pierce, B. M.; Brédas, J. L. *J. Am. Chem. Soc.* **1994**, *116*, 10703.
- Bourhill, G.; Brédas, J.-L.; Cheng, L.-T.; Marder, S. R.; Meyers, F.; Perry, J. W.; Tiemann, B. G. *J. Am. Chem. Soc.* **1994**, *116*, 2619.
- Marder, S. R.; Perry, J. W.; Bourhill, G.; Gorman, C. B.; Tiemann, B. G.; Mansour, K. *Science* **1993**, *261*, 186.
- Marder, S. R.; Perry, J. W.; Tiemann, B. G.; Gorman, C. B.; Gilmour, S.; Biddle, S. L.; Bourhill, G. *J. Am. Chem. Soc.* **1993**, *115*, 2524.
- (43) Winget, P.; Weber, E. J.; Cramer, C. J.; Truhlar, D. G. *Phys. Chem. Chem. Phys.* **2000**, *2*, 1231.
- Jonsson, M.; Houmam, A.; Jocy, G.; Wayner, D. D. M. *J. Chem. Soc., Perkin Trans. 2* **1999**, 425.
- (44) Facchetti, A.; Mushrush, M.; Katz, H. E.; Marks, T. J. *Adv. Mater.* **2003**, *15*, 33.
- (45) Huang, H.; Pickup, P. G. *Chem. Mater.* **1998**, *10*, 2212.